A Reliable Automated Synthesis of 6-[18F]Fluoro-L-DOPA and the Clinical Application on the Imaging of Congenital Hyperinsulinism of Infants

Zhengwei Zhang
Fudan University School of Pharmacy
Jingjie Ge
Huashan Hospital Fudan University
Kai Jing
East China University of Science and Technology School of Pharmacy
Yefeng Chen
East China University of Science and Technology School of Pharmacy
Yihui Guan
Huashan Hospital Fudan University
Hexin Xie (xiehexin@ecust.edu.cn)
East China University of Science and Technology School of Pharmacy https://orcid.org/0000-0003-1033-9211
Jianhua Zhu
Fudan University School of Pharmacy

Research Article

Keywords: 6-[18F]fluoro-L-DOPA, radiosynthesis, positron emission tomography, congenital hyperinsulinism, imaging

Posted Date: January 3rd, 2022

DOI: https://doi.org/10.21203/rs.3.rs-1218396/v1

Version of Record: A version of this preprint was published at Medicinal Chemistry Research on February 5th, 2022. See the published version at https://doi.org/10.1007/s00044-022-02850-w.

Abstract

6-[^{18}F]fluoro-L-DOPA is a radiotracer widely used in the diagnosis of a range of diseases, including neuro-oncology, endocrinology, and Parkinson's disease. To meet the fast growing clinical need for this radioactive compound, this study reports an optimized radiosynthsis of this molecule, which proved to be highly reliable and compatible with different types of automated radiosynthesizers. Moreover, with 6-[^{18}F]fluoro-L-DOPA, the PET/CT imaging of a total of 23 patients has been conducted, further demonstrating this radiotracer as a clinically valuable reagent to diagnose congenital hyperinsulinism (CHI) of infancy and, more importantly, localize the exact lesion on pancreas.

Introduction

Positron emission tomography (PET), which allows imaging the physiological processes of human being in a noninvasive manner, has become a highly important technique for disease diagnosis [1, 2]. The implementation of PET imaging relies on radio-active PET tracers, positron-emitting radionuclides-labeling bioactive molecules or radiopharmaceuticals. And thus a reliable and automated synthesis of PET tracers has been critical for PET imaging.

6-[^{18}F]fluoro-L-DOPA [3], since its first clinical application in the imaging of dopaminergic pathways of human brain [4], has been used to report a wide variety of diseases [5], including neuro-oncology [6, 7], endocrinology [8], and Parkinson's disease [9, 10], As a result, a range of methods have been developed for this valuable radiotracer.[11, 12] The first synthesis of radioactive L-DOPA (5-[^{18}F]fluoro-L-DOPA) was accomplished by Firnau and co-workers in 1973 using diazonium fluoroborate compound as precursor [13]. The same lab later reported the synthesis of this radiotracer by the reaction of L-DOPA and [^{18}F]F_2, which afforded only a mixture of 2-, 5- and [^{18}F]fluoro-L-DOPA [14]. Benzaldehydes containing a leaving group, such as nitro [15] and quaternary ammonium salt [16, 17], have also been employed as radiofluorination precursors and 6-[^{18}F]fluoro-L-DOPA was obtained after a few steps. Nevertheless, the requirement of a multiple-step chemical transformations of radioactive molecules makes these approaches less feasible in automated radiosynthesis. Enantiomerically pure organostannane [18, 19], organosilane [20], or organomercury [21], has been reported to give 6-[^{18}F]fluoro-L-DOPA in a two-step process up treatment with electrophilic [^{18}F]F_2 or [^{18}F]AcOF. Nevertheless, these electrophilic reagents are less accessible and specialized settings are requisite in these processes. Enantiomerically pure diaryliodonium salt, on the other hand, allows the synthesis of 6-[^{18}F]fluoro-L-DOPA with nucleophilic [^{18}F]KF, but in poor radiochemical yield (RCY) [22].

In 2014, the Gouverneur lab developed a copper-mediated radiofluorination ofBPin precursorwith [^{18}F]KF as fluorination source [23]. On the basis of this approach, 6-[^{18}F]fluoro-L-DOPA could be readily synthesized in two steps from precursor **1a** (Scheme 1) [23, 24]. Soon after that, aryl- and vinylboronicacids were reported to be compatible with the copper-mediated radiofluorination [25]. In spite of these tremendous progresses, to meet the rapidly increasing clinical need for 6-[18F]fluoro-L-DOPA in

oncology, neurology, and endocrinology, a highly reliable, time-saving, and automated synthesizer-compatible radiosynthetic approach for this tracer is still in high demand. Herein, we report a copper-promoted automated synthesis of 6-[^{18}F]fluoro-L-DOPA with high reliability and, more importantly, the clinical applications of this radiotracer in the diagnosis of congenital hyperinsulinism (CHI) of infancy, which, to the best of our knowledge, is the first clinical investigation of 6-[^{18}F]fluoro-L-DOPA in the diagnosis of CHI in China.

Results And Discussion

We initially commenced our investigation by testing the copper-mediated radiofluorination of BPin-substituted L-DOPA (**1a**) [23]. Following this protocol, we managed to obtain clinically useful amount of 6-[18F]fluoro-L-DOPA, though in lower radiochemical yield compared to original study. Nevertheless, the use of highly corrosive hydroiodic acid (57%) in the final deprotection reaction resulted in significant damage on the sealing ring of automated synthesizer (Fig. 1a); replacement of this part was needed after a few attempts of syntheses. Moreover, the injection loop of HPLC was blocked occasionally during the purification of this radioactive molecule with RP-HPLC. We reasoned this is likely due to the formation of water-insoluble iodine during the final deprotection, which might be resulted from the oxidation of hydroiodic acid by oxygen or other oxidants. As the radiosynthesis of tracer is a highly time-sensitive process, the frequent occurrence of these issues significantly jeopardizes the reliability of this ^{18}F-labelling approach.

To tackle these challenges, we then moved to employ BPin-substituted L-DOPA **1b** as precursor, in which methoxymethyl (MOM, R^1) and *tert*-butyl (R^2) were selected as protecting groups [26]. We conceived the use of this more acid-sensitive precursor should allow the final deprotection using hydrochloric acid, instead of problematic hydroiodic acid (Scheme 1).

As shown in Scheme 2, precursor **1b** was readily synthesized from commercially available L-DOPA by a 6-step process [27]. With this precursor, we then conducted the standard copper-mediated radiofluorination and resulted in the ^{18}F-labelling intermediate in comparable radiochemical yield based on HPLC analysis, suggesting the replacement of protecting groups has little impact on this reaction. Subsequently treating this radioactive intermediate with hydrochloric acid (6 M) at 120 ^{o}C led to complete removal of all protecting groups in 20 minutes. The overall radiochemical yield of 6-[^{18}F]Fluoro-L-DOPA is similar to the fluorination with **1a** as precursor. And, more importantly, we observed no damage on the sealing ring (Fig. 1b) or blocking of injection loop during this process, which enhances the synthetic reliability of 6-[^{18}F]Fluoro-L-DOPA.

Nonetheless, further testing of this copper-mediated protocol revealed the synthetic yields fluctuated greatly, ranging from 1.7 to 8.7%RCY (decay uncorrected, Table 1). This promoted us to conduct further investigations to improvethis radiosynthetic process. We soon realized the fluctuation of yield might associate with the salt in the eluent for $^{18}F^{-}$ before the copper-mediated radiofluorination. As a result, we

replaced potassium carbonate with potassium oxalate in the eluent for $^{18}F^-$ and the yield was boosted to 13.02 ± 3.3% RCY. (n = 10, decay uncorrected, Table 1). The whole process, including radiosynthesis and purification, took approximately 85 minutes and, most of the time, the yields were higher than 10% (RCY, decay uncorrected). Upon analysis by HPLC (Fig. 2), the radiochemical purity of 6-[^{18}F]Fluoro-L-DOPA was better than 99%, which should meet the clinical need for this important PET radiotracer.

Table 1

Effect of the salts in the eluent for 18F$^-$ on the radiosynthesis of 6-[^{18}F]Fluoro-L-DOPA

entry	elution of $^{18}F^-$ with K_2CO_3 in H_2O		elution of $^{18}F^-$ with $K_2C_2O_4$ in H_2O	
	Radioactivity of prod. (mCi)	RCY (%)[a]	Radioactivity of prod. (mCi)	RCY (%)[a]
1	25	2	140	11.4
2	83	6.8	200	16.3
3	21	1.7	236	19.2
4	22	1.8	146	11.9
5	54	4.4	153	12.5
6	107	8.7	105	8.6
7	73	5.9	170	13.8
8	21	1.7	163	13.3
9	76	6.2	184	15
10	53	4.3	101	8.2

a. decay uncorrected.

To further assess the compatibility of this radioflurination protocol, we then examined it on two types of commercial automated radiosynthesizers: RNplus (Synthra GmbH Company, Germany) and PET-MF-2V-IT-1 (Beijing PET Technology Co., Ltd, China) (Fig. 3). After a number of tests, both synthesizers gave desired radiotracer in comparable yields, demonstrating the high compatibility of this radiosynthetic method.

Congenital hyperinsulinism (CHI), the inappropriate secretion of insulin by the pancreatic β-cells, is among the major causes for severe hypoglycemia in infants [28]. Rapid diagnosis of CHI is of high importance because the presence of abnormal level of insulin may lead to seizure and significant brain damage or even death [29]. PET imaging with 6-[^{18}F]Fluoro-L-DOPA as radiotracer has been reported as

an important approach to diagnose CHI with high accuracy [30–32]. Having confirmed purity of 6-[^{18}F]Fluoro-L-DOPA and the reliability of this automated synthesis protocol, we next turned our attention to the diagnosis of CHI in infants or young kids using this radiotracer.

Upon approval by the Institutional Review Board of Huashan Hospital (HIRB), Fudan University, the first patient tested with 6-[^{18}F]Fluoro-L-DOPA is an infant girl at the age of 9 months, who had repeated episodes of hypoglycemia since birth and a significant increase in serum insulin (25.1 IU/mL). However, neither magnetic resonance (MR) imaging nor computed tomography (CT) scan found the exact lesions on the patient (Fig. 3). The patient was thus administered with 1.2 mCi of 6-[^{18}F]Fluoro-L-DOPA and scanned with PET/CT at 60 minutes' post-injection. As shown in Fig. 3, we observed strong radiation signal from the head of patient's pancreas, indicating significantly higher uptake of L-DOPA by these pancreatic β-cells. On the basis of these data, this patient was diagnosed to have focal forms of CHI (FoCHI). Fortunately, upon selective resection of pancreatic tissue (2 cm) proximal to the uncinated process by laparoscopic surgery, the patient recovered to normal level of blood glucose at the second day after surgery.

Encouraged by these results, a total of 23 children (13 boys and 10 girls) diagnosed with CHI were tested with 6-[^{18}F]Fluoro-L-DOPA. These patients were at an average age of 15.4 ± 21.3 months, ranging from 2 to 78 months (Table 2). All of these patients under fasting state showed: 1) insulin was still secreted abnormally even when the blood glucose was lower than 2.6 mmol/L; 2) the blood glucose increased more than 1.5 mmol/L in the islet glucagon provocation test; 3) the adrenocortical hormone, growth hormone and thyroid function were at normal level at hypoglycemia; 4) the tests of blood- and urine-ketone were negative; 5) the analysis of blood by LC-MS and urine by GC-MS were negative. Upon injection of 6-[^{18}F]Fluoro-L-DOPA, all of these children showed strong radiation signal at pancreas in PET/CT images. As summarized in Table 1, 7 patients showed focal abnormal increase of uptake of 6-[^{18}F]Fluoro-L-DOPA in the pancreas (FoCHI): 5 of them were located in the head of the pancreas, 1 in the body of pancreas and 1 in the tail of pancreas. Moreover, 4 of the 7 patients with FoCHI have received surgery or pathological biopsy of the pancreas and the results are all consistent with the PET/CT images.

The other 16 children also showed higher uptake of 6-[^{18}F]Fluoro-L-DOPA in pancreas, but in a diffuse manner, indicating these patients have diffuse forms of CHI (DiCHI). These results manifest a proximally 30% of tested patients have focal lesions (FoCHI) while about 70% of patients have DiCHI. These numbers are close to the results of clinical studies carried out in the western child population, which reported that the proportion of FoCHI accounts for about 33% - 35% of all children with CHI [31]. This study, to the best of our knowledge, is the first clinical investigation of 6-[^{18}F]Fluoro-L-DOPA-based PET imaging in the diagnosis of CHI in China. These results in our study further demonstrate 6-[^{18}F]Fluoro-L-DOPA as a highly valuable tracer of PET, not only in the diagnosis of CHI but also in the localization of the exact lesion of CHI.

Table 2
Clinical profile of 23 patients with CHI

entry	gender	age (months)	weight (kg)	results based on PET images of ^{18}F-FDOPA	pathological biopsy
1	M	9	9	FoCHI (pancreas head)	Yes
2	M	3	7.5	FoCHI (pancreastail)	Yes
3	M	2	6.5	FoCHI (pancreas head)	Yes
4	M	2	6.5	DiCHI	Yes
5	M	2	5.5	DiCHI	Yes
6	F	2	6	FoCHI (pancreas head)	Yes
7	F	8	6	DiCHI	No
8	M	18	14	DiCHI	No
9	M	2	6.5	DiCHI	No
10	F	2	7	DiCHI	No
11	F	2	6	DiCHI	No
12	F	2	6	FoCHI (pancreas head)	No
13	M	18	11	DiCHI	No
14	F	5	10	FoCHI (pancreas head)	No
15	M	2	6.5	FoCHI (pancreasbody)	No
16	M	5	9	DiCHI	No
17	F	4	9.5	DiCHI	No
18	M	48	17	DiCHI	No
19	M	54	17	DiCHI	No
20	F	49	14	DiCHI	No
21	F	28	22	DiCHI	No
22	M	10	10	DiCHI	No
23	F	78	30	DiCHI	No

Conclusions

In summary, we report herein a copper-mediated automated synthesis of 6-[^{18}F]fluoro-L-DOPA from BPin-substituted precursor. Upon a serial of optimizations, this radiofluorination protocol proved to be compatible with different types of automated radiosynthesizers, affording clinically valuable 6-[^{18}F]fluoro-L-DOPA in good radiochemical yields and, more significantly, with high reliability. The implementation of this protocol should make this imaging reagent more accessible for clinic investigation. Moreover, this radiotracer has been clinically applied in PET imaging for the diagnosis of CHI on 23 patients, which led to comparable results as previous studies. These results further demonstrate 6-[^{18}F]fluoro-L-DOPA as a highly clinically important tracer to diagnose CHI and localize exact lesion on pancreas. Under the guidance of the 6-[^{18}F]fluoro-L-DOPA-based PET/CT imaging, a number of patients have undergone surgical intervention and recovered from abnormal level of blood glucose. This study, to the best of our knowledge, is the first clinical investigation of 6-[^{18}F]fluoro-L-DOPA-based PET imaging for CHI in China.

Materials And Methods

General Information

Unless otherwise stated, all chemicals were obtained from commercial sources and used without further purification. The ^{1}H and ^{13}C NMR spectra were taken on Bruker nuclear magnetic resonance spectrometer. Chemical shifts are reported as δ in units of parts per million (ppm) relative to internal standard (^{1}H NMR: $SiMe_4$ = 0.00 ppm). Data for ^{1}H NMR spectra are reported as follows: chemical shifts are reported as δ in units of parts per million (ppm) relative to tetramethylsilane (δ = 0, s); multiplicities are reported as follows: s (singlet), d (doublet), t (triplet), q (quartet), dd (doublet of doublets), m (multiplet), or br (broadened); coupling constants are reported as a *J* value in Hertz (Hz); the number of protons (n) for a given resonance is indicated nH, and based on the spectral integration values. High-performance liquid chromatography (HPLC) analysis and purification was performed on a waters HPLC system equipped with a SPD UV detector, a LC pump system, and a CBM BUS module. A Lablogic Scan-RAM radio-HPLC detector was used for the radioactive signal. Water containing 0.1% acetic acid/sodium acetate and 0.2 g/L ascorbic acid) was filtered before use as HPLC mobile phase. HPLC purification of 6-[^{18}F]fluoro-L-DOPA was performed on a semi-preparative reversed-phase Phenomenex Gemini column (Phenomenex, Luna, C18(2), 5 μ, ,250 mm · 10 mm) with method A (flow rate: 5 mL min^{-1}). Analysis of 6-[^{18}F]fluoro-L-DOPA was performed on a reversed-phase analytical Phenomenex column (Phenomenex, Lu, a□C18(2), 5 μm, 250 mm · 4.6 mm) with Method B (flow rate: 1 mL min^{-1}).

Synthesis Of Precursor 1b

tert **-Butyl** (S)**-2-amino-3-(3,4-dihydroxyphenyl)propanoate (2)**

Under argon atmosphere, to a solution of L-DOPA (2.96 g, 15 mmol) in *tert*-butyl acetate (30 mL, 225 mmol) at 0 ^{o}C was added $HClO_4$ (70% in H_2O, 1.9 mL, 22 mmol). The resulting mixture were stirred overnight, allowing the reaction temperature raise to room temperature. Upon completion of the reaction, water was added and the pH of solution was adjusted to 8 with a 10% aqueous solution of K_2CO_3. The organic phase was separated and the aqueous phase was extracted with DCM (60 mL × 3). The combined organic layers were dried over Na_2SO_4 and purified by chromatography on a silica gel column to afford titled compound as a yellow liquid (1.62 g, 42%). ^{1}H NMR (400 MHz, $CDCl_3$) δ 6.72 (d, *J* = 7.9 Hz, 1H), 6.56 (d, *J* = 2.0 Hz, 1H), 6.55 (dd, *J* = 8.0, 1.7 Hz, 1H), 4.34 (s, 4H), 3.62 (dd, *J* = 8.2, 4.7 Hz, 1H), 3.01 (dd, *J* = 13.8, 4.7 Hz, 1H), 2.72 (dd, *J* = 13.9, 8.4 Hz, 1H), 1.49 (s, 9H).

tert **-Butyl (** S **)-2-((** tert **-butoxycarbonyl)amino)-3-(3,4-dihydroxyphenyl) propan-oate (3)**

Under argon atmosphere, to a solution of **2** (0.77 g, 3 mmol) in EtOH (15 mL) at room temperature was added Boc_2O (0.68 g, 3 mmol). The resulting mixture were stirred at room temperature for 5 h. After the solvent was removed via Rota-Vap, the residue was purified by chromatography on a silica gel column (PE/EA = 3/1) to afford titled compound a white solid (0.8 g, 74%). ^{1}H NMR (400 MHz, $CDCl_3$) δ 6.74 (d, *J* = 6.3 Hz, 1H), 6.70 (s, 1H), 6.56 (d, *J* = 8.1 Hz, 1H), 6.33 (s, 1H), 6.15 (s, 1H), 5.06 (d, *J* = 11.8 Hz, 1H), 4.38 (q, *J* = 14.0, 6.5 Hz, 1H), 2.99 – 2.84 (m, 1H), 1.41 (s, 1H).

tert **-Butyl (S)-3-(3,4-bis(methoxymethoxy)phenyl)-2-((** tert **-butoxycarbonyl)amino) propanoate (4)**

Under argon atmosphere, to a solution of **3** (562 mg, 1.6 mmol) in DCM (8 mL) at 0 ^{o}C were added DIPEA (0.7 ml, 4 mmol) and DMAP (20 mg, 0.16 mmol). The reaction mixture was stirred at the same temperature for 10 min, then MOMCl (0.3 mL, 4 mmol) was added dropwise. The resulting mixture were then heated to reflux for 20 h. After cooling to room temperature, water was then added and the aqueous phase was extracted with DCM. The combined organic layers were washed by a 10% aqueous solution of K_2CO_3 and dried over Na_2SO_4 and purified by chromatography on a silica gel column (PE/EA = 10/1) to afford titled compound as a colorless liquid (477 mg, 68%). ^{1}H NMR (400 MHz, $CDCl_3$) δ 7.07 (d, *J* = 8.3 Hz, 1H), 6.97 (s, 1H), 6.76 (d, *J* = 8.3 Hz, 1H), 5.21 (s, 4H), 4.98 (d, *J* = 8.0 Hz, 1H), 4.42 (dd, *J* = 13.5, 6.1 Hz, 1H), 3.51 (s, 6H), 2.99 (d, *J* = 4.7 Hz, 2H), 1.42 (s, 18H). ^{13}C NMR (101 MHz, $CDCl_3$) δ 170.96, 155.07, 147.08, 146.15, 130.66, 123.50, 118.06, 116.53, 95.45, 81.99, 79.63, 56.16, 54.70, 37.79, 28.32, 27.96.

tert **-Butyl (S)-2-((** tert **-butoxycarbonyl)amino)-3-(2-iodo-4,5-bis(methoxymethoxy) phenyl)propanoate (5)**

Under argon atmosphere, to a solution of **4** (450 mg, 1.02 mmol) in DCM (anhydrous, 20 mL) at 0 ^{o}C were added [Bis(trifluoroacetoxy)iodo]benzene (526 mg, 1.224 mmol) and I_2 (260 mg, 1.02 mmol). The reaction mixture was stirred for 3 h, allowing the reaction temperature raised to room temperature. Upon completion of the reaction (monitored by TLC), the reaction was quenched by an aqueous solution of Na_2SO_3. The organic layer was separated and the aqueous phase was extracted with DCM. The combined organic layers were dried over Na_2SO_4 and purified by chromatography on a silica gel column

(PE/EA = 10/1) to afford titled compound as a colorless liquid (399 mg, 69%). ^{1}H NMR (400 MHz, $CDCl_3$) δ 7.56 (s, 1H), 7.03 (s, 1H), 5.19 (s, 4H), 5.03 (d, *J* = 8.7 Hz, 1H), 4.51 (q, *J* = 14.7, 8.6 Hz, 1H), 3.50 (s, 6H), 3.16 (dd, *J* = 14.0, 5.6 Hz, 1H), 2.95 (dd, *J* = 13.9, 9.1 Hz, 1H), 1.43 (s, 9H), 1.38 (s, 9H). ^{13}C NMR (101 MHz, $CDCl_3$) δ 171.06, 155.02, 147.36, 146.56, 133.87, 126.86, 118.24, 95.44, 91.23, 81.99, 79.61, 56.30, 54.08, 42.99, 28.28, 27.96.

tert **-Butyl (S)-3-(4,5-bis(methoxymethoxy)-2-(4,4,5,5-tetramethyl-1,3,2-dioxaborolan-2-yl)phenyl)-2-((** tert **-butoxycarbonyl)amino)propanoate (6)**

Under argon atmosphere, to a solution of bis(pinacolato)diboron (139.7 mg, 0.55 mmol), $Pd(dppf)Cl_2.CH_2Cl_2$ (20.4 mg, 0.025 mmol) and CH_3COOK (147 mg,1.5 mmol) in DMF (anhydrous, 20 mL) at room temperature was added **5** (284 mg, 0.5 mmol). The reaction mixture was heated to 80 ^{o}C for 18 h. After cooling to room temperature, a saturated aqueous solution of NaCl was added, followed by ethyl acetate. The organic layer was separated and the aqueous phase was extracted with ethyl acetate (50 mL×3). The combined organic layers were then dried over Na_2SO_4 and purified by chromatography on a silica gel column (PE/EA = 15/1) to afford titled compound as a colorless liquid (166 mg, 58%). ^{1}H NMR (400 MHz, $CDCl_3$) δ 7.51 (s, 1H), 7.05 (s, 1H), 5.94 (d, *J* = 8.2 Hz, 1H), 5.26 (m, 4H), 4.17 (m, 1H), 3.53 (s, 3H), 3.50 (s, 3H), 3.30 – 2.95 (m, 2H), 1.47 (s, 9H), 1.37 (s, 6H), 1.36 (s, 6H), 1.34 (s, 9H).

tert **-Butyl (S)-3-(4,5-bis(methoxymethoxy)-2-(4,4,5,5-tetramethyl-1,3,2-dioxa borolan-2-yl)phenyl)-2-((di** tert **-butoxycarbonyl)amino)propanoate (1b)**

Under argon atmosphere, to a solution of **6** (61 mg, 0.11 mmol) in MeCN (anhydrous, 0.8 mL) at room temperature were added Boc_2O (240 mg, 1.1 mmol), DMAP (13.7 mg, 0.11 mmol) and Et_3N (46 µl, 0.33 mmol). The reaction mixture were heated to 40 ^{o}C for 24 h. After cooling to room temperature, the solvent was removed via Rota-Vap and ethyl acetate (100 mL) was added. The organic phase was then washed by a saturated aqueous solution of NH_4Cl, dried over Na_2SO_4 and purified by chromatography on a silica gel column (PE/EA = 15/1) to afford titled compound as a yellow liquid (56 mg, 78%). ^{1}H NMR (400 MHz, $CDCl_3$) δ 7.49 (s, 1H), 6.88 (s, 1H), 5.28 – 5.11 (m, 5H), 3.93 (dd, *J* = 13.4, 3.7 Hz, 1H), 3.50 (s, 3H), 3.46 (s, 3H), 3.03 (t, 1H), 1.50 (s, 9H), 1.36 (s, 18H), 1.33 (s, 6H), 1.31 (s, 6H). ^{13}C NMR (101 MHz, $CDCl_3$) δ 169.46, 151.98, 149.44, 144.56, 140.59, 124.05, 118.88, 95.39, 95.11, 83.42, 82.14, 80.82, 60.86, 56.09, 35.02, 27.73, 24.90.

Radiosynthesis Of 6-[f]fluoro-l-dopa

Noncarrier-added [^{18}F]fluoride was obtained via the $^{18}O(p,n)^{18}F$ nuclear reaction on a RDS111 cyclotron using enriched $H_2{}^{18}O$. A QMA cartridge was eluted to a reaction vessel with an aqueous solution of Kryptofix 222 and $K_2C_2O_2$ and the solvent was dried azeotropically at 110 ℃ under N_2. Acetonitrile (anhydrous, 2 mL) was added and dried at 110℃ under N_2. A solution of **1b** (20 mg) and $Cu(OTf)_2(py)_4$

(20 mg) in DMF (0.8 mL) were added and the mixture were heated to 120 ℃ for 20 minutes. Then the reaction mixture were cooled down and diluted with water (8 mL). The resulting mixture were transfer to a C18 cartridge and washed with water (8 mL). The compounds in the C18 cartridge were thus eluted with acetone (3 mL) to another reaction vessel and the volatile solvent was removed by heating to 110℃ under N_2. HCl (aq. 6 M) was then added and the reaction solution was heated to 120 ℃ for 20 minutes. Then was reaction mixture was cooled down and diluted with a NaOH (aq. 0.1M, 5 mL). 6-[^{18}F]fluoro-L-DOPA was obtained after purification by HPLC on a C18 column with water containing 0.1% acetic acid/sodium acetate and 0.2 g/L ascorbic acid as eluent (flow rate = 5 mL/min, tR = 8.9 min).

Pet/ct Scanning

This study was approved by the Institutional Review Board of Huashan Hospital (HIRB), Fudan University, China. All patients were administered intravenously 0.08 to 0.16 mCi/kg of [^{18}F]fluoro-L-DOPA was administered intravenously. A 10 min/bed abdominal static emission scan was acquired 60-70 minutes after injection with a PET/CT scanner (Siemens Biograph 64 HD PET/CT, Siemens, Germany). Attenuation correction was performed using a low-dose CT (30-40mAs, 120 kV, Acq. 32×1.2 mm) before the emission scan. Following corrections for scatter, dead time, and random coincidences, PET images were reconstructed by TrueX+TOF with 4 iterations and 21 subsets, a Gaussian Filter (FWHM 4.0 mm).

Declarations

Acknowledgement

We are grateful for financial support from the National Natural Science Foundation of China (81571345), the Shanghai Committee of Science and Technology (14DZ1930400, 14DZ1930402), and the Research Center on Aging and Medicine, Fudan University (IDF151006)

Conflict of Interest

The authors declare no competing interests.

References

1. Ametamey SM, Honer M, Schubiger PA (2008) Molecular imaging with PET. Chem Rev 108(5):1501–1516. doi:10.1021/cr0782426
2. Duclos V, Iep A, Gomez L, Goldfarb L, Besson FL (2021) PET Molecular Imaging: A Holistic Review of Current Practice and Emerging Perspectives for Diagnosis, Therapeutic Evaluation and Prognosis in Clinical Oncology. Int J Mol Sci 22(8):4159. doi:10.3390/ijms22084159
3. Taieb D, Imperiale A, Pacak K (2016) (18)F-DOPA: the versatile radiopharmaceutical. Eur J Nucl Med Mol Imaging 43(6):1187–1189. doi:10.1007/s00259-016-3354-0

4. Garnett ES, Firnau G, Nahmias C (1983) Dopamine visualized in the basal ganglia of living man. Nature 305(5930):137–138. doi:10.1038/305137a0
5. Nanni C, Fanti S, Rubello D (2007) 18F-DOPA PET and PET/CT. J Nucl Med 48(10):1577–1579. doi:10.2967/jnumed.107.041947
6. Heiss WD, Wienhard K, Wagner R, Lanfermann H, Thiel A, Herholz K et al (1996) F-Dopa as an amino acid tracer to detect brain tumors. J Nucl Med 37(7):1180–1182
7. Nandu H, Wen PY, Huang RY (2018) Imaging in neuro-oncology. Ther Adv Neurol Disord 11:1756286418759865. doi:10.1177/1756286418759865
8. Santhanam P, Taieb D (2014) Role of (18) F-FDOPA PET/CT imaging in endocrinology. Clin Endocrinol 81(6):789–798. doi:10.1111/cen.12566
9. Darcourt J, Schiazza A, Sapin N, Dufour M, Ouvrier MJ, Benisvy D et al (2014) 18F-FDOPA PET for the diagnosis of parkinsonian syndromes. Q J Nucl Med Mol Imaging 58(4):355–365
10. Ibrahim N, Kusmirek J, Struck AF, Floberg JM, Perlman SB, Gallagher C et al (2016) The sensitivity and specificity of F-DOPA PET in a movement disorder clinic. Am J Nucl Med Mol Imaging 6(1):102–109
11. Andersen VL, Soerensen MA, Dam JH, Langkjaer N, Petersen H, Bender DA et al (2021) GMP production of 6-[(18)F]Fluoro-L-DOPA for PET/CT imaging by different synthetic routes: a three center experience. EJNMMI Radiopharm Chem 6(1):21. doi:10.1186/s41181-021-00135-y
12. Neves ACB, Hrynchak I, Fonseca I, Alves VHP, Pereira MM, Falcao A et al (2021) Advances in the automated synthesis of 6-[(18)F]Fluoro-L-DOPA. EJNMMI Radiopharm Chem 6(1):11. doi:10.1186/s41181-021-00126-z
13. Firnau G, Nahmias C, Garnett S (1973) The preparation of [18F]5-Fluoro-DOPA with reactor-produced fluorine-18. Int J Appl Radiat Isot 24(3):182–184
14. Firnau G, Chirakal R, Garnett ES (1984) Aromatic radiofluorination with [18F]fluorine gas: 6-[18F]fluoro-L-dopa. J Nucl Med 25(11):1228–1233
15. Kaneko S, Ishiwata K, Hatano K, Omura H, Ito K, Senda M (1999) Enzymatic synthesis of no-carrier-added 6-[18F]fluoro-L-dopa with beta-tyrosinase. Appl Radiat Isot 50(6):1025–1032. doi:10.1016/s0969-8043(98)00173-0
16. Lemaire C, Damhaut P, Plenevaux A, Comar D (1994) Enantioselective synthesis of 6-[fluorine-18]-fluoro-L-dopa from no-carrier-added fluorine-18-fluoride. J Nucl Med 35(12):1996–2002
17. Libert LC, Franci X, Plenevaux AR, Ooi T, Maruoka K, Luxen AJ et al (2013) Production at the Curie level of no-carrier-added 6-18F-fluoro-L-dopa. J Nucl Med 54(7):1154–1161. doi:10.2967/jnumed.112.112284
18. Namavari M, Bishop A, Satyamurthy N, Bida G, Barrio JR (1992) Regioselective radiofluorodestannylation with [18F]F2 and [18F]CH3COOF: a high yield synthesis of 6-[18F]Fluoro-L-dopa. Int J Rad Appl Instrum A 43(8):989–996. doi:10.1016/0883-2889(92)90217-3

19. Fuchtner F, Angelberger P, Kvaternik H, Hammerschmidt F, Simovc BP, Steinbach J (2002) Aspects of 6-[18F]fluoro-L-DOPA preparation: precursor synthesis, preparative HPLC purification and determination of radiochemical purity. Nucl Med Biol 29(4):477–481. doi:10.1016/s0969-8051(02)00298-6
20. Diksic M, Farrokhzad S (1985) New synthesis of fluorine-18-labeled 6-fluoro-L-dopa by cleaving the carbon-silicon bond with fluorine. J Nucl Med 26(11):1314–1318
21. Chaly T, Bandyopadhayay D, Matacchieri R, Belakhleff A, Dhawan V, Takikawa S et al (1994) A disposable synthetic unit for the preparation of 3-O-methyl-6-[18F]fluorodopa using a regioselective fluorodemercuration reaction. Appl Radiat Isot 45(1):25–30. doi:https://doi.org/10.1016/0969-8043(94)90143-0
22. Edwards R, Westwell AD, Daniels S, Wirth T (2015) Convenient Synthesis of Diaryliodonium Salts for the Production of [18F]F-DOPA. Eur J Org Chem 2015(3):625–630. doi:10.1002/ejoc.201403378
23. Tredwell M, Preshlock SM, Taylor NJ, Gruber S, Huiban M, Passchier J et al (2014) A general copper-mediated nucleophilic 18F fluorination of arenes. Angew Chem Int Ed 53(30):7751–7755. doi:10.1002/anie.201404436
24. Preshlock S, Calderwood S, Verhoog S, Tredwell M, Huiban M, Hienzsch A et al (2016) Enhanced copper-mediated (18)F-fluorination of aryl boronic esters provides eight radiotracers for PET applications. Chem Commun 52(54):8361–8364. doi:10.1039/c6cc03295h
25. Mossine AV, Brooks AF, Makaravage KJ, Miller JM, Ichiishi N, Sanford MS et al (2015) Synthesis of [18F]Arenes via the Copper-Mediated [18F]Fluorination of Boronic Acids. Org Lett 17(23):5780–5783. doi:10.1021/acs.orglett.5b02875
26. During the course of our study, a similar synthetic approach has been reported see: a), Mossine AV, Tanzey SS, Brooks AF, Makaravage KJ, Ichiishi N, Miller JM, Henderson BD, Skaddan MB, Sanford MS, Scott PJH, Mossine AV, Tanzey SS, Brooks AF, Makaravage KJ, Ichiishi N, Miller JM, Henderson BD, Erhard T, Bruetting C, Skaddan MB, Sanford MS, Scott PJH (2019) Synthesis of high-molar-activity [(18)F]6-fluoro-L-DOPA suitable for human use via Cu-mediated fluorination of a BPin precursor, Nat. Protoc., 15 (2020) 1742-1759
27. Jing K (2016) Study on the synthesis of 6-[18F]F-L-DOPA, master's thesis, East China University of Science and Technology,
28. Arnoux JB, Verkarre V, Saint-Martin C, Montravers F, Brassier A, Valayannopoulos V et al (2011) Congenital hyperinsulinism: current trends in diagnosis and therapy. Orphanet J Rare Dis 6:63. doi:10.1186/1750-1172-6-63
29. Chinoy A, Banerjee I, Flanagan SE, Ellard S, Han B, Mohamed Z et al (2019) Focal Congenital Hyperinsulinism as a Cause for Sudden Infant Death. Pediatr Dev Pathol 22(1):65–69. doi:10.1177/1093526618765376
30. Dubois J, Brunelle F, Touati G, Sebag G, Nuttin C, Thach T et al (1995) Hyperinsulinism in children: diagnostic value of pancreatic venous sampling correlated with clinical, pathological and surgical outcome in 25 cases. Pediatr Radiol 25(7):512–516. doi:10.1007/BF02015782

31. Ribeiro MJ, De Lonlay P, Delzescaux T, Boddaert N, Jaubert F, Bourgeois S et al (2005) Characterization of hyperinsulinism in infancy assessed with PET and 18F-fluoro-L-DOPA. J Nucl Med 46(4):560–566
32. Hardy OT, Hernandez-Pampaloni M, Saffer JR, Scheuermann JS, Ernst LM, Freifelder R et al (2007) Accuracy of [18F]fluorodopa positron emission tomography for diagnosing and localizing focal congenital hyperinsulinism. J Clin Endocrinol Metab 92(12):4706–4711. doi:10.1210/jc.2007-1637

Schemes

Schemes 1 and 2 are available in the Supplemental Files section

Figures

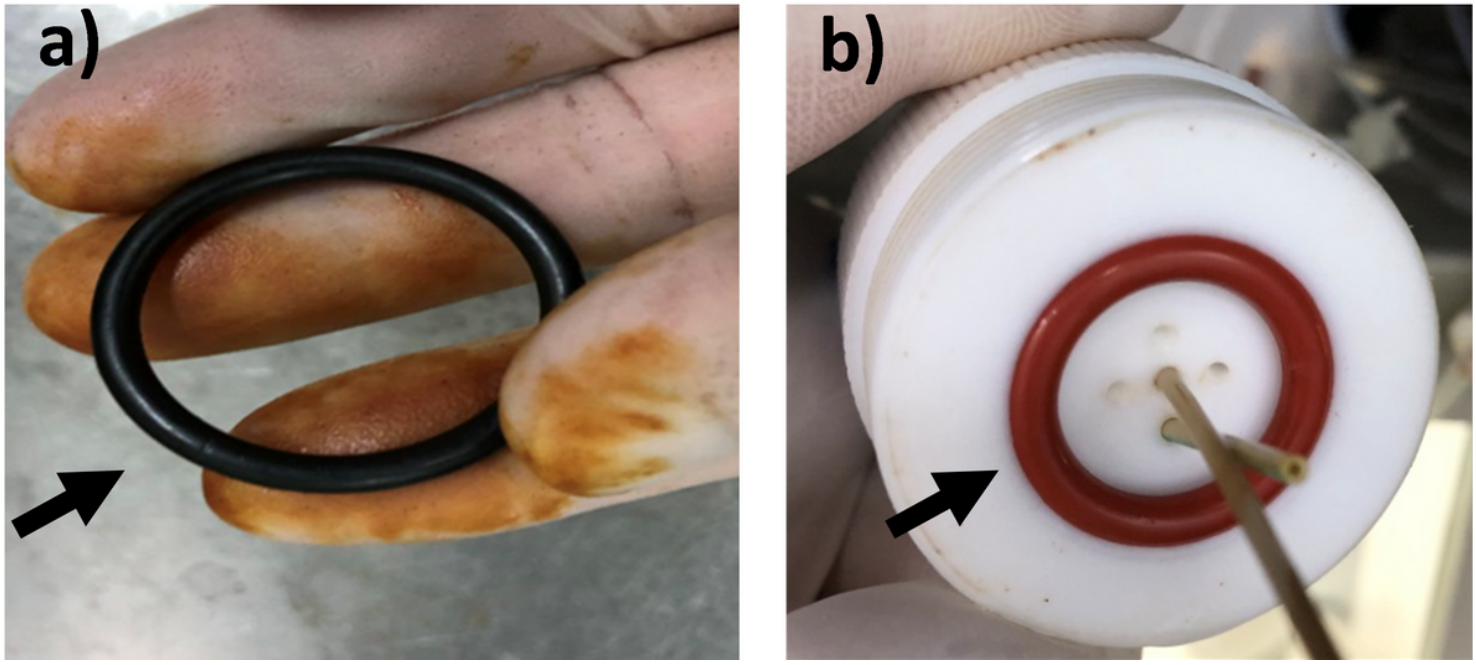

Figure 1

Sealing rings of automated synthesizers after radiosyntheses of 6-[^{18}F]Fluoro-L-DOPA using HI (57%, **a**) and HCl (6 M, **b**)

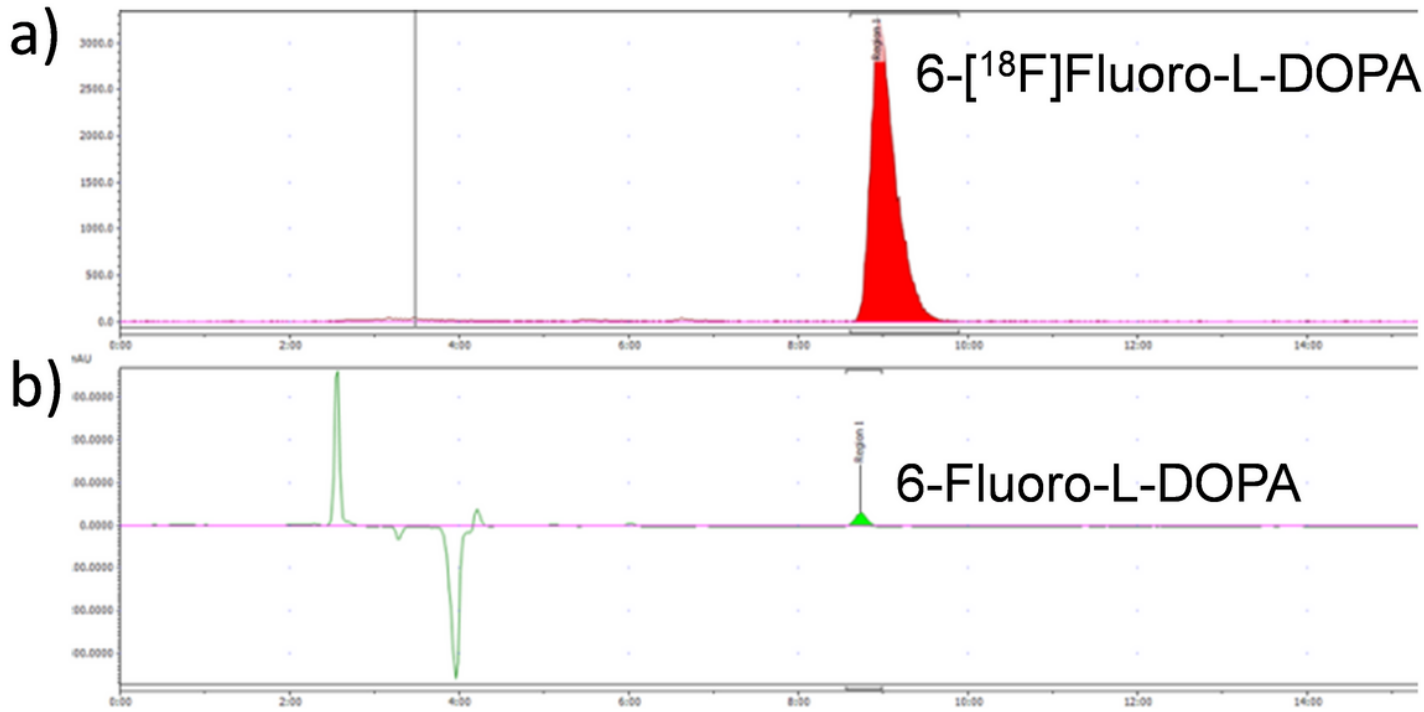

Figure 2

HPLC chromatograms of 6-[^{18}F]Fluoro-L-DOPA. a) Radio-HPLC for 6-[^{18}F]Fluoro-L-DOPA. b) UV-HPLC for ^{19}F-standard compound.

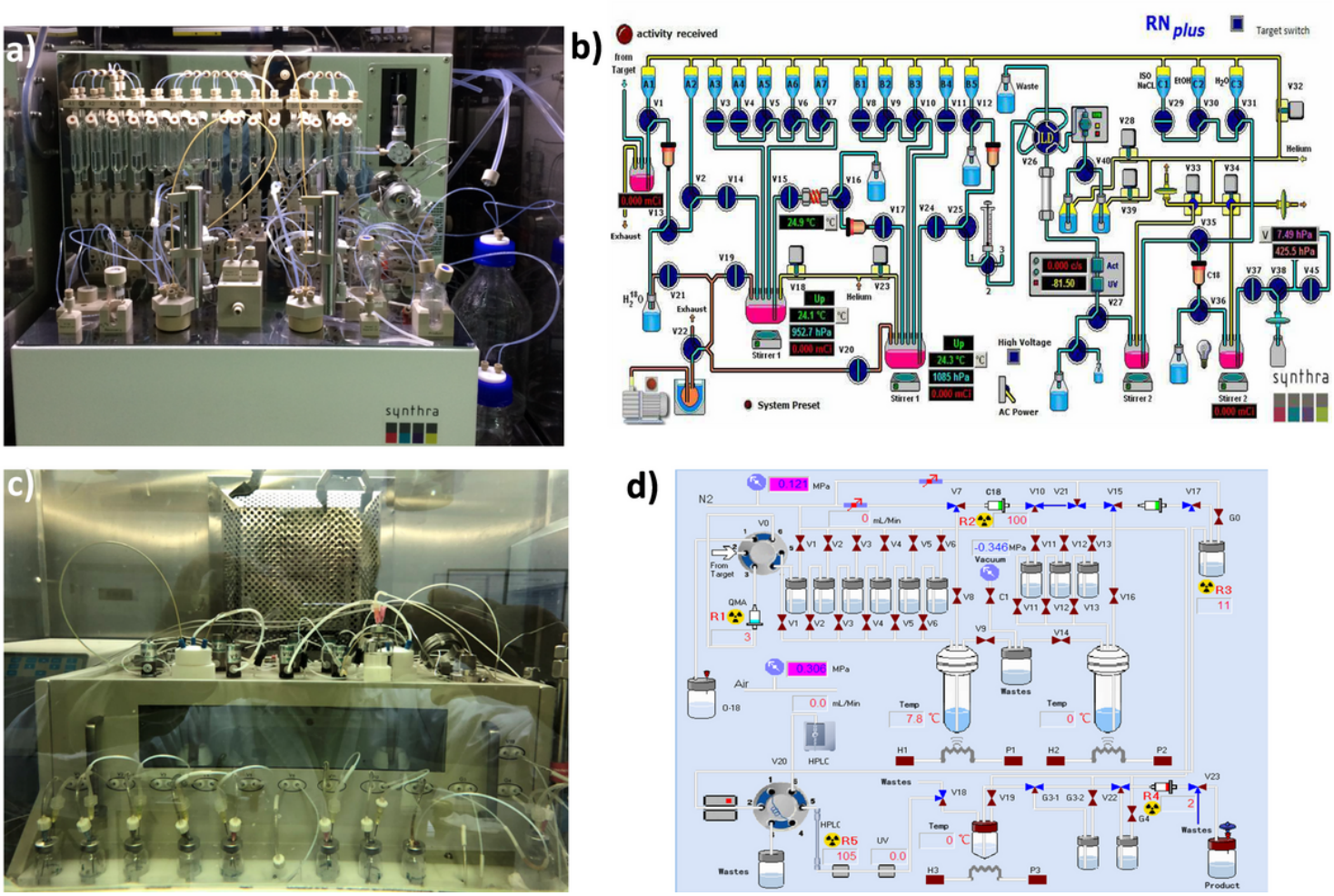

Figure 3

The automated radiosynthesizers and their synthesis modules used in this study. **a**) and **b**): RNplus automated radiosynthesizer; **c**) and **d**): ET-MF-2V-IT-1 automated radiosynthesizer

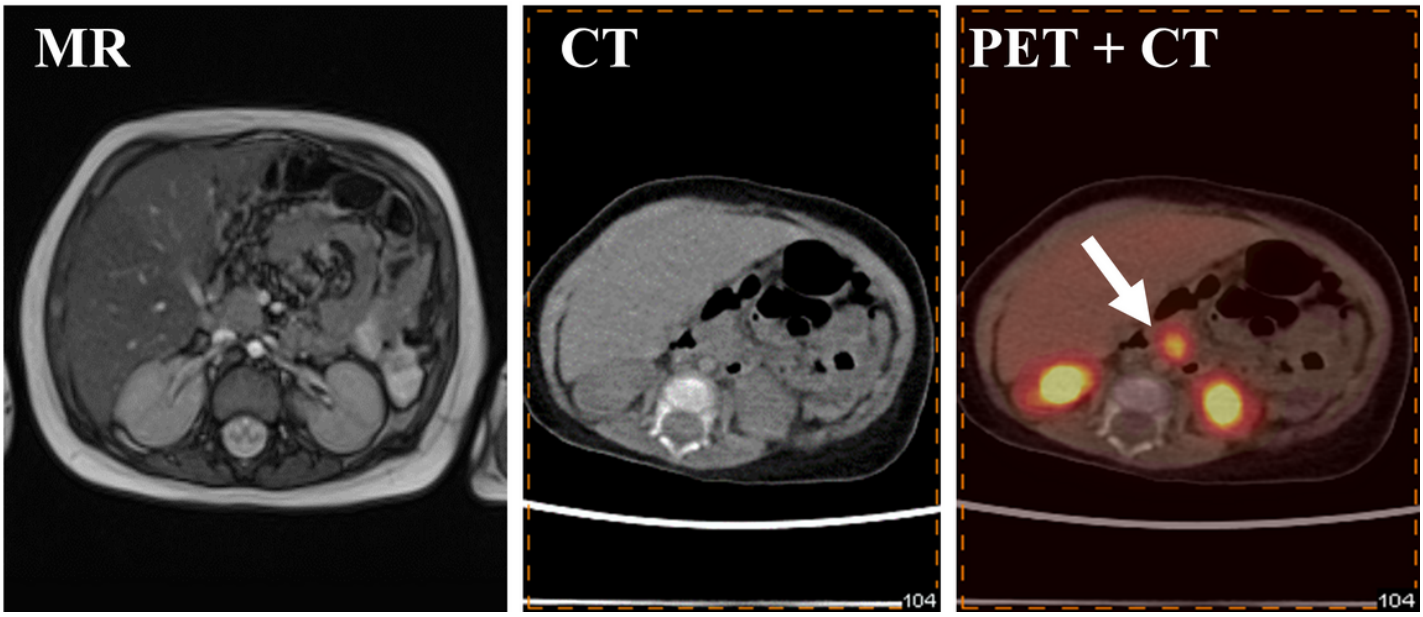

Figure 4

MR, CT, and PET/CT images of a patient with CHI. The arrow points to the lesion on pancreas

Supplementary Files

This is a list of supplementary files associated with this preprint. Click to download.

- GraphicalA.png
- Scheme1.png
- Scheme2.png
- SupportingInformation.docx